



Effect of partial substitution of Cr³⁺ for Fe³⁺ on magnetism, magnetocaloric effect and transport properties of Ba₂FeMoO₆ double perovskites

M. El-Hagary^{a,b,*}

^a Physics Department, Faculty of Science, Helwan University, Helwan, Cairo, Egypt

^b Institut für Festkörperphysik, TU Wien, A-1040 Wien, Austria

ARTICLE INFO

Article history:

Received 23 February 2010

Received in revised form 14 April 2010

Accepted 24 April 2010

Available online 5 May 2010

PACS:

75.30.Sg

82.80.-d

Keywords:

Magnetocaloric effect

Double perovskite

Magnetic properties

Transport properties

ABSTRACT

Magnetism, magnetocaloric effect and transport properties of Cr doped double perovskites compound Ba₂Fe_{1-x}Cr_xMoO₆ with (0 ≤ x ≤ 1) were investigated by magnetization and electrical resistivity measurements. The samples show a cubic structure of cell parameter, *a*, decreases with increasing Cr content. The temperature variation in magnetization reveals a ferromagnetism for all samples with *T_c* decreases significantly as the Cr doping content increases from 340 K to 310 K for x = 0 and 1, respectively. The saturation magnetic moment, *μ_s*, was found to decrease with increasing the Cr doped content from 3.63 *μ_B*/f.u. for x = 0 to 2.69 *μ_B*/f.u. for x = 1 which may relate to the increase of the anti-site disorder defects or magnetic dilution due to the substitution of Cr for Fe. The magnetocaloric effect is calculated from the measurement of initial isothermal magnetization versus magnetic field at various temperatures. The maximum magnetic entropy change, |Δ*S_M*^{max}|, of Cr doped double perovskite is found to decrease with increasing of Cr content from 2.08 J/kg K for x = 0 to 0.55 J/kg K for x = 1 upon 1 T applied field change. Interestingly, the value of |Δ*S_M*^{max}| = 2.08 J/kg K for x = 0 at 1 T was found to be about 64% that of pure Gd, which is thought to be the optimum magnetic refrigerant for use near room temperature. Thus, this perovskite is beneficial for the household application of active magnetic refrigerant materials. The zero field electrical resistivity measurements exhibit a change from metallic behavior at x = 0 to semiconducting like behavior for all doped samples (x ≥ 0.2) over the entire measurement temperature region from 4.2 K to 300 K.

© 2010 Elsevier B.V. All rights reserved.

1. Introduction

The double perovskite half metals have recently been the object of extensive research due to the exotic physics and potential spintronic applications [1]. The chemical formula is A₂BB'O₆, where A is alkaline ion, and B and B' are different transition metal cations [2–4]. The crystal structure of the double perovskite can be viewed as a regular arrangement of corner-sharing BO₆ and B'O₆ octahedra alternating along the three directions of the crystal, with the large A cations occupying the voids in between the octahedra. Depending on the relative size of the B and B' cations with respect to the A cations, the crystal structure can be occurred as cubic (with space group *Fm3m*), tetragonal (*I4/mmm*) or monoclinic (*P2₁/n*) [5,6]. The double perovskite with two ordered B-site cations are ferromagnetic for B = Cr, Fe, Co... and B' = Mo, Re, W, U... [7,8]. Magnetic behavior comes from antiferromagnetic coupling among localized 3d⁵ electrons of high spin ion at B-site and itinerant 4d electrons

of ion at B'site [9]. Moreover, the interest in the double perovskites is the discovery of colossal magnetoresistance (CMR) properties at temperatures above room temperature in Sr₂FeMoO₆ which is significantly higher than for any mixed-valence manganite [10]. Further interest for the double perovskite has also been driven by possible technological applications of these materials in magnetoelectronic devices. In general, the interesting physical properties of the double perovskites are primarily due to the electronic interactions of B-site cations. Thus, small chemical substitutions on B and/or B' can lead to change the magnetic properties and a distortion of the structures of the double perovskites that are correlated with their electronic properties. For example, in most studied compound, Sr₂FeMoO₆, partial or complete substitutions onto the Fe site is a useful method to probe the physics because the magnetic and electronic properties are critically dependent on the exchange splitting of the Fe₂(t_{2g}) and (e_g) orbitals [11]. On the other hand, several authors have investigated the effect of a number of substitutions on B and/or B'sites in the double perovskite on structural, magnetic, transport, magneto-transport, and magnetocaloric properties [11–18]. To our knowledge, no studies have carried on the magnetocaloric effect (MCE) of the Ba₂Fe_{1-x}Cr_xMoO₆ double perovskite.

* Current address: Physics Department, College of Science, Qassim University, P.O. Box 6644, 51452 Buryadh, Saudi Arabia. Tel.: +966 6 3800319; fax: +966 6 3801581. E-mail address: magelhagary@gmail.com.

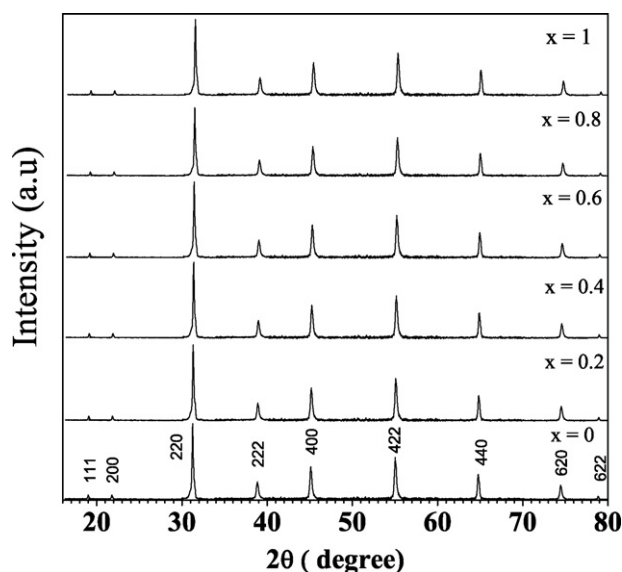


Fig. 1. X-ray diffraction patterns of $\text{Ba}_2\text{Fe}_{1-x}\text{Cr}_x\text{MoO}_6$ ($0 \leq x \leq 1$) systems.

In this paper we attempt to synthesize $\text{Ba}_2\text{Fe}_{1-x}\text{Cr}_x\text{MoO}_6$ double perovskite samples with $x = 0, 0.2, 0.4, 0.6, 0.8, 1$ to investigate the magnetocaloric effect with different Cr doping concentration on the B (Fe^{3+}) site. In addition, the magnetic and transport properties upon a partial disorder of Cr on the B-site of $\text{Ba}_2\text{Fe}_{1-x}\text{Cr}_x\text{MoO}_6$ double perovskite samples are also investigated.

2. Experimental details

A series of polycrystalline samples of $\text{Ba}_2\text{Fe}_{1-x}\text{Cr}_x\text{MoO}_6$ ($x = 0, 0.2, 0.4, 0.6, 0.8, 1$) were synthesized by a conventional solid state reaction method. Stoichiometric amounts of high-purity analytical grade (99.99% or better) BaCO_3 , Fe_2O_3 , MoO_3 , and Cr_2O_3 were mixed and ground in an agate mortar for about four hours. The mixed powders were calcined at 900°C in Ar atmosphere for 10 h with intermediate grindings and pelletizations. The calcined mixed powders were pressed into pellets. The pellets were then sintered at 1200°C for 10 h in a gas flow of 5% H_2 and 95% Ar. The final disk-shape samples are obtained after a very slow cooling process from the sintering to room temperature.

The structure and phase purity of the samples were checked at room temperature by means of X-ray powder diffraction (XRD) Shimadzu Diffractometer XRD 6000, Japan, with $\text{Cu-K}\alpha_1$ radiation ($\lambda = 1.54056 \text{ \AA}$). The data were collected by step-scan modes in a 2θ range between 15° and 80° with step-size of 0.02° and step time of 0.6 s. Pure Silicon (~ Si 99.9999%) was used as an internal standard. The magnetic measurements in the temperature range 1.8–400 K with a frequency of 40 Hz were performed on a quantum design vibrating sample magnetometer PPMS-6000 VSM. Resistivity was measured by four-probe DC technique.

3. Results and discussion

3.1. Structural characterization

X-ray diffraction (XRD) studies for $\text{Ba}_2\text{Fe}_{1-x}\text{Cr}_x\text{MoO}_6$ ($0 \leq x \leq 1$) samples at room temperature exhibited an almost single phase samples without detectable secondary phase (see Fig. 1). The XRD patterns were indexed on the basis of the cubic structure with a space group $Fm\bar{3}m$. As can be seen in Fig. 1 no structure transi-

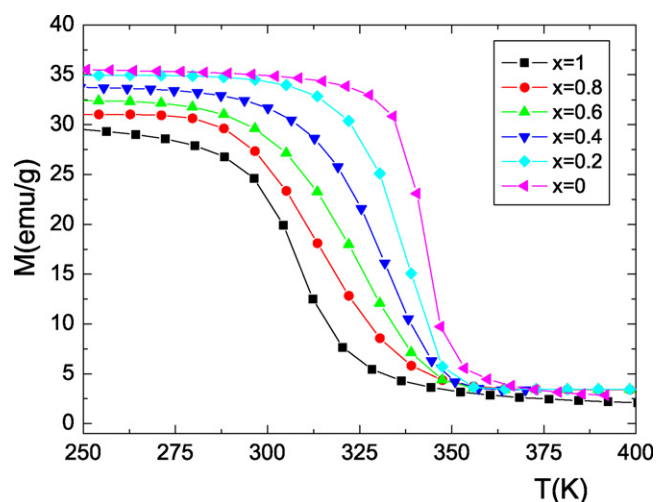


Fig. 2. Temperature dependence of magnetization, $M(T)$, for $\text{Ba}_2\text{Fe}_{1-x}\text{Cr}_x\text{MoO}_6$ ($0 \leq x \leq 1$) measured at applied magnetic field of 1 T.

tion has been observed on substituting Fe/Cr over the entire Cr range. This is in agreement with the crystallography results of the previously studied $\text{Ba}_2\text{CrMo}_{1-x}\text{W}_x\text{O}_6$ double perovskite [16]. They reported that a partial substitution of $\text{W}^{5+,6+}$ by $\text{Mo}^{5+,6+}$ on the B-site indicates change of average ionic radius without distortion of the crystal symmetry. The lattice parameters of $\text{Ba}_2\text{Fe}_{1-x}\text{Cr}_x\text{MoO}_6$ ($0 \leq x \leq 1$) obtained with the method of least square refinement are summarized in Table 1. The results show a continuous decrease in the lattice constant with increasing Cr content in the samples ($a = 8.061 \text{ \AA}$ for $\text{Ba}_2\text{FeMoO}_6$ and $a = 8.013 \text{ \AA}$ for $\text{Ba}_2\text{CrMoO}_6$) which is obvious due to smaller ionic radius of Cr^{3+} (0.615 \AA) compared to ionic radius of Fe^{3+} (0.645 \AA). The lattice parameter values of parent compounds are in good agreement with lattice parameters of $\text{Ba}_2\text{FeMoO}_6$ and $\text{Ba}_2\text{CrMoO}_6$ reported in literatures [16,19].

3.2. Magnetic properties

The temperature dependence of magnetization measurements, $M(T)$, of the double perovskite $\text{Ba}_2\text{Fe}_{1-x}\text{Cr}_x\text{MoO}_6$ ($0 \leq x \leq 1$) at 1 T are shown in Fig. 2. The curves reveal paramagnetic (PM) to ferromagnetic (FM) phase transition at Curie temperature, T_C . The Curie temperatures, T_C , of the samples were determined from the temperature at which dM/dT curve reaches a maximum in the magnetization versus temperature (under low magnetic field) representations, see Table 1. Apparently, the ferromagnetic transition decreases significantly as the Cr doping content increases, from 340 K for $x = 0$ to 310 K for $x = 1$. This reduction in T_C is principally a consequence of combined effects of the chemical pressure [20], carrier doping and anti-site disorder defects [21]. Due to smaller ionic radius of Cr, the substitution of Cr in place of Fe increases the chemical pressure in the lattice. As a result the orbital overlap and exchange coupling changes. Nevertheless, the presence of (Fe,Cr)/Mo disorder due to anti-site defects was the main origin of destroying the ferromagnetic state, and leads to a decrease of T_C .

Table 1

Unit cell parameter, magnetic, magnetocaloric and transport data of $\text{Ba}_2\text{Fe}_{1-x}\text{Cr}_x\text{MoO}_6$ ($0 \leq x \leq 1$).

x	a (Å)	T_C [K]	μ_S (at 20 K) [$\mu_B/\text{f.u.}$]	$ \Delta S_M^{\text{max}} $ ($\mu_0 H = 1 \text{ T}$) [J/kg K]	ρ (at 300 K) ($\Omega \text{ cm}$)	ρ (at 10 K) ($\Omega \text{ cm}$)
0	8.061(2)	340(5)	3.63	2.09	4.60×10^{-4}	2.64×10^{-5}
0.2	8.051(1)	338(5)	3.48	1.20	4.79×10^{-3}	3.91×10^{-2}
0.4	8.042(2)	333(5)	3.30	0.86	7.40×10^{-3}	8.71×10^{-2}
0.6	8.032(3)	325(5)	3.10	0.70	8.60×10^{-3}	1.10×10^{-1}
0.8	8.022(3)	316(5)	2.88	0.63	1.02×10^{-2}	1.30×10^{-1}
1	8.013(2)	310(5)	2.69	0.55	2.10×10^{-3}	2.68×10^{-2}

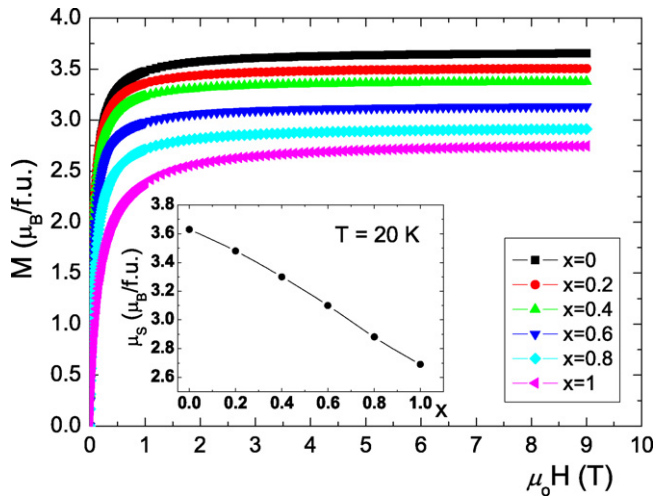


Fig. 3. Magnetization curves for $\text{Ba}_2\text{Fe}_{1-x}\text{Cr}_x\text{MoO}_6$ ($0 \leq x \leq 1$) at 20 K under an external field up to 9 T; the inset shows the saturated magnetic moment versus the Cr content, x .

The T_C value at $x=0$ is similar to that of $\text{Ba}_2\text{FeMoO}_6$ sample reported by Zhong et al. [14]. Furthermore, the magnetization decreases gradually with the increasing of small amounts of Cr doping (Fig. 2).

The field dependence of the magnetization for $\text{Ba}_2\text{Fe}_{1-x}\text{Cr}_x\text{MoO}_6$ samples ($x=0, 0.2, 0.4, 0.6, 0.8$ and 1) at 20 K under an external field up to 9 T is displayed in Fig. 3. The results reveal that the saturation magnetic moment, μ_S , of $\text{Ba}_2\text{Fe}_{1-x}\text{Cr}_x\text{MoO}_6$ double perovskite ($0 \leq x \leq 1$) compounds decreases as Cr doping content increases from $3.63 \mu_B/\text{f.u.}$ for $x=0$ to $2.69 \mu_B/\text{f.u.}$ for $x=1$, see the inset of Fig. 3. This is confirmed with the fact that the Cr^{3+} saturation moment is expected to be smaller than the Fe^{3+} saturation moment. The significant decrease of the saturation magnetic moment with x might be attributed to the increase of the anti-site disorder defects [22,23] or magnetic dilution due to the substitution of Cr for Fe. The values of μ_S for pure compounds are in good agreement of those values reported in literatures [14,19]. It is worth noting that the observed value of the saturation magnetic moment for $\text{Ba}_2\text{FeMoO}_6$ double perovskite lies slightly below the theoretical value of $4 \mu_B/\text{f.u.}$ of the fully ordered $\text{Ba}_2\text{FeMoO}_6$ double perovskite. This reduction is principally a consequence of Fe/Mo anti-site disorder [22–24]. According to Ogale et al. [23] the saturation magnetic moment of $3.7 \mu_B/\text{f.u.}$ corresponds to an anti-site disorder of 2.4% in the Fe and Mo sites.

3.3. Magnetocaloric effect

Some intermetallic compounds and alloys of heavy rare earths with a large magnetic moment, such as Gd and $\text{Gd}_5\text{Ge}_2\text{Si}_2$ have been proposed to be good candidates for magnetic refrigeration applications at room temperature [25,26]. Additionally, the large magnetic entropy changes of rare earth intermetallic compounds $\text{RT}_{13-x}\text{M}_x$ (R=rare earth, T=Co, Fe and M=Si, Al) obtained at a relatively low field make these intermetallic compounds are possible candidates for magnetic refrigerant materials, see e.g. Ref. [27]. Furthermore, several authors have investigated the magnetocaloric effect in ABO_3 type perovskite manganites and found their magnetic entropy change is comparable to that of Gd [28–32]. However, to our knowledge little results have been reported on the MCE of the double perovskite transition oxide [14–16]. Here, we study the effect of Cr doping at B-site (Fe) in the polycrystalline $\text{Ba}_2\text{Fe}_{1-x}\text{Cr}_x\text{MoO}_6$ ($0 \leq x \leq 1$) double perovskite on the magnetocaloric properties.

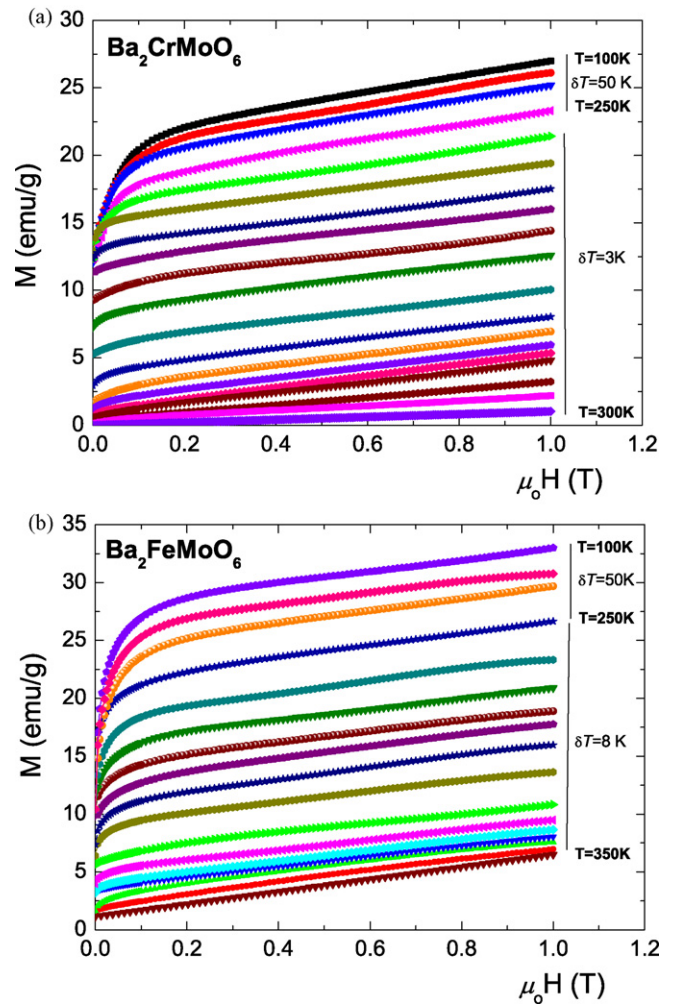


Fig. 4. Isothermal magnetization versus magnetic field obtained at different temperatures under an external field up to 1 T for $\text{Ba}_2\text{Fe}_{1-x}\text{Cr}_x\text{MoO}_6$ (a) sample with $x=1$ and (b) sample with $x=0$.

The magnetic entropy change can be measured either by the adiabatic change of temperature under the application of a magnetic field or through the measurement of initial isothermal magnetization versus magnetic field at various temperatures. In this study, the second method was used to avoid the difficulties of adiabatic measurements.

According to classical thermodynamic theory, the magnetic entropy change ΔS_M due to the variation of the external magnetic field from 0 to maximum field H is written as:

$$\Delta S_M(T, H) = \int_0^H \left(\frac{\partial M}{\partial T} \right)_H dH' \quad (1)$$

For magnetization measured at discrete field and temperature intervals, the magnetic entropy change ΔS_M can be approximated as:

$$|\Delta S_M| = \sum_i \frac{M_i - M_{i+1}}{T_{i+1} - T_i} \Delta H \quad (2)$$

where M_i and M_{i+1} are the experimental values of the magnetization obtained at the temperatures T_i and T_{i+1} , respectively, under the magnetic field H . The change of magnetic field ΔH – i.e. the difference between the minimal and maximal external magnetic field applied – in our case is equal to H (because the minimum field was set to 0).

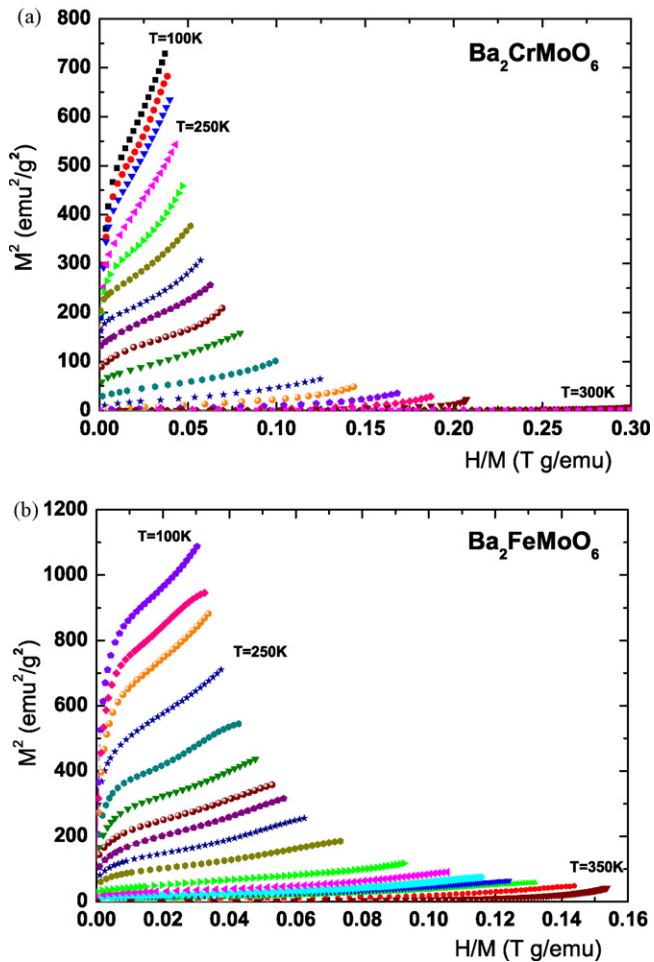


Fig. 5. The M^2 versus H/M plots at different temperatures for $\text{Ba}_2\text{Fe}_{1-x}\text{Cr}_x\text{MoO}_6$ (a) sample with $x=1$ and (b) sample with $x=0$.

Isothermal magnetization, (M – H), curves are obtained around the Curie temperature of samples. Fig. 4(a and b) shows an example of such curves for the end member samples ($x=0, 1$) of $\text{Ba}_2\text{Fe}_{1-x}\text{Cr}_x\text{MoO}_6$ compound measured over a wide temperature range under an external field up to 1 T. The temperature step is 3 K, 8 K in the range from 250 K to temperature above 300 K for samples with $x=0$ and 1, respectively and 50 K for the others temperature ranges. Obviously, the magnetization has been found to increase with decreasing temperature in the temperature range 100–350 K, where thermal fluctuation of spins decreases with decreasing temperature. The nature of the magnetic phase transition in the Cr doped investigated compounds has been examined by using Banerjee criterion [33]. According to which the slope of M^2 versus H/M curves (Arrott plot) denotes whether the observed magnetic phase transition is of the first order (negative slope) or, second order (positive slope). A typical set of M^2 versus H/M curves for the end compositions ($x=0$ and 1) of $\text{Ba}_2\text{Fe}_{1-x}\text{Cr}_x\text{MoO}_6$ compound is depicted in Fig. 5(a and b). Clearly, the Arrott plots obtained for all the $\text{Ba}_2\text{Fe}_{1-x}\text{Cr}_x\text{MoO}_6$ ($0 \leq x \leq 1$) samples indicate positive slope in their complete M^2 versus H/M curves and confirm the transition to be the second order.

Based on Eq. (2), the magnetic entropy changes as a function of temperature, for all samples, at external magnetic field of 1 T were calculated. The temperature dependence of the magnetic entropy change, $|\Delta S_M|$, as a function of temperature under an applied field of 1 T for $\text{Ba}_2\text{Fe}_{1-x}\text{Cr}_x\text{MoO}_6$ double perovskite samples with $x=0, 0.2, 0.4, 0.6, 0.8$ and 1 is shown in Fig. 6. As expected from Eq. (2)

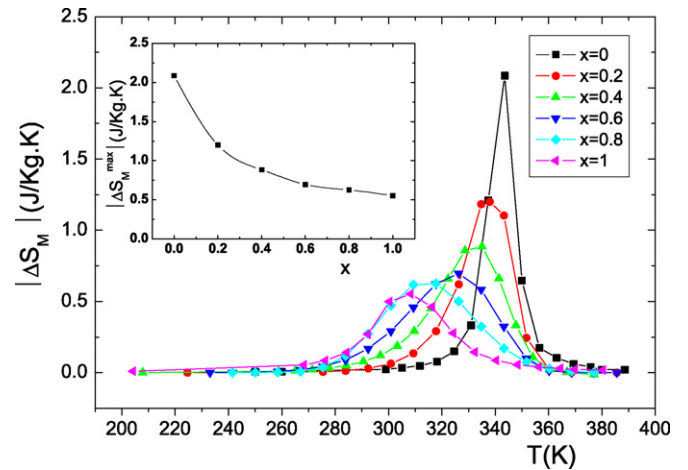


Fig. 6. Temperature dependence of the magnetic entropy change $|\Delta S_M|$ at the magnetic applied field change of $\mu_0 H = 1$ T for $\text{Ba}_2\text{Fe}_{1-x}\text{Cr}_x\text{MoO}_6$ ($0 \leq x \leq 1$); the inset shows the variation of maximum entropy change with the Cr content, x .

the maximum values of $|\Delta S_M|$, i.e. $|\Delta S_M^{\max}|$, are obtained around each Curie temperature T_C . It is obvious that the maximum entropy change is rather large, $|\Delta S_M^{\max}| = 2.08$ J/kg K, for $\text{Ba}_2\text{Fe}_{1-x}\text{Cr}_x\text{MoO}_6$ with $x=0$ upon 1 T external applied field change. Moreover, as the Cr doping content increase, maximum entropy change $|\Delta S_M^{\max}|$ decreases (see Table 1) and the curves of the magnetic entropy changes become broader. The broadening in the magnetic entropy change due to Cr^{3+} substitution can be explained as follows: when small amounts of Cr^{3+} doped in $\text{Ba}_2\text{FeMoO}_6$ the magnetic transition becomes broader and broader due to Cr^{3+} substitution, so gives rise to a larger broadening of the magnetic entropy change. It has been shown that the large magnetic entropy change in perovskite results mainly from the considerable variation of magnetization near T_C [34–36]. The spin–lattice coupling in the magnetic ordering process also plays an important role in additional magnetic entropy change near T_C , and consequently, enhances the MCE [35,36]. Therefore, the large magnetic entropy change in the present perovskites $\text{Ba}_2\text{Fe}_{1-x}\text{Cr}_x\text{MoO}_6$ ($0 \leq x \leq 1$) compounds can originate from the abrupt reduction of magnetization, which is associated with a FM to PM phase transition in the vicinity of Curie temperature T_C . Namely, spin alignments induced by magnetic field led to negative entropy change. Furthermore, the sharper the change in magnetization at T_C the larger magnetic entropy change obtained (see Fig. 6). However, the decrease of the magnetic entropy changes with increasing of the Cr doping at the B-site could be caused by the change of the double exchange interaction [37,38]. In order to make a comparison of the maximum entropy change values for these samples with those reported in literatures for several materials considered

Table 2

Magnetocaloric properties obtained for $\text{Ba}_2\text{Fe}_{1-x}\text{Cr}_x\text{MoO}_6$ ($0 \leq x \leq 1$) compounds compared with different materials.

Sample	T_C [K]	$\mu_0 H$ [T]	$ \Delta S_M^{\max} $ [J/kg K]	Reference
$\text{Ba}_2\text{FeMoO}_6$	340	1	2.09	Present work
$\text{Ba}_2\text{Fe}_{0.8}\text{Cr}_{0.2}\text{MoO}_6$	338	1	1.20	Present work
$\text{Ba}_2\text{Fe}_{0.6}\text{Cr}_{0.4}\text{MoO}_6$	333	1	0.86	Present work
$\text{Ba}_2\text{Fe}_{0.4}\text{Cr}_{0.6}\text{MoO}_6$	325	1	0.70	Present work
$\text{Ba}_2\text{Fe}_{0.2}\text{Cr}_{0.8}\text{MoO}_6$	316	1	0.63	Present work
$\text{Ba}_2\text{CrMoO}_6$	310	1	0.55	Present work
Gd	292	1	3.25	[39]
$\text{Ba}_2\text{FeMoO}_6$	340	1	1.54	[14]
$\text{Ba}_2\text{CrMoO}_6$	335	1	1.26	[16]
$\text{La}_{0.77}\text{Sr}_{0.23}\text{Mn}_{0.8}\text{Cu}_{0.2}\text{O}_3$	293	1	2.68	[28]
$\text{La}_{0.67}\text{Ca}_{0.275}\text{Sr}_{0.055}\text{MnO}_3$	285	1	2.80	[29]
$\text{La}_{0.67}\text{Ca}_{0.33}\text{MnO}_3$	260	1	1.20	[40]

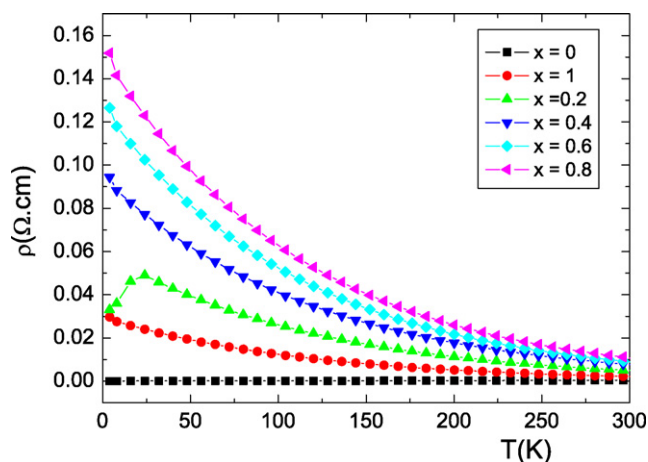


Fig. 7. Resistivity under zero applied magnetic field as a function of temperature for $\text{Ba}_2\text{Fe}_{1-x}\text{Cr}_x\text{MoO}_6$ ($0 \leq x \leq 1$).

promising for magnetic refrigeration we have collected the different $|\Delta S_M^{\text{max}}|$ values in Table 2. One should be noted that the value of the maximum entropy changes for $\text{Ba}_2\text{Fe}_{1-x}\text{Cr}_x\text{MoO}_6$ with $x=0$ sample above 300 K at 1 T is found to be 25% higher than that for $\text{Ba}_2\text{FeMoO}_6$ sample under a field change of 1 T reported by Zhong et al. [14]. However, our value of the maximum entropy change for $\text{Ba}_2\text{Fe}_{1-x}\text{Cr}_x\text{MoO}_6$ with $x=1$ under field change of 1 T is lower than that value reported by Dhahri et al. [16] for $\text{Ba}_2\text{CrMoO}_6$ under a field change of 1 T. Furthermore, it is important to see also from Table 2 that the value of $|\Delta S_M^{\text{max}}|$ obtained in the $\text{Ba}_2\text{Fe}_{1-x}\text{Cr}_x\text{MoO}_6$ with $x=0$ sample is about 64% that of pure Gd, which is thought to be the optimum magnetic refrigerant for use near room temperature. In addition, when compared with Gd and its alloys [39], the present perovskites are easier to fabricate, possess a higher chemical stability and their T_C can be adjusted by tuning the doping concentration. Finally, it is interesting to note that the large magnetic entropy changes were found to occur around 300 K, allowing room temperature magnetic refrigeration. This result indicates that the present double perovskite samples especially at $x \leq 0.4$ are of practical importance, because it could be good working materials for magnetic refrigeration in household refrigerators.

3.4. Electrical transport properties

Fig. 7 depicts the temperature dependence of the zero field resistivity $\rho(T)$ of $\text{Ba}_2\text{Fe}_{1-x}\text{Cr}_x\text{MoO}_6$ ($0 \leq x \leq 1$) compounds. It can be seen that both parent compounds have a very low resistivity. The $\rho(T)$ curves exhibit a change from metallic behavior ($d\rho/dT < 0$) at $x=0$ to semiconducting like behavior ($d\rho/dT > 0$) for all doped samples ($x \geq 0.2$) over the entire measurement temperature region from 4.2 K to 300 K. Furthermore, the resistivity increases by some order of magnitude with the increase of the Cr content. The resistivities at room temperature (300 K) are $4.6 \times 10^{-4} \Omega \text{ cm}$ and $2.1 \times 10^{-3} \Omega \text{ cm}$ for $x=0$ and 1, respectively, whereas the resistivities are $4.79 \times 10^{-3} \Omega \text{ cm}$, $7.4 \times 10^{-3} \Omega \text{ cm}$, $8.6 \times 10^{-3} \Omega \text{ cm}$ and $1.02 \times 10^{-2} \Omega \text{ cm}$ for $x=0.2, 0.4, 0.6$ and 0.8 , respectively. It should be noted that the resistivity of the sample with $x=0.2$ shows a shallow peak at low temperatures. Accordingly, we can see a charge localization and destruction of the metallic behavior of the Cr doping. The carriers are localized over the entire composition range ($0 \leq x \leq 1$) although the existence of ferromagnetic exchange and ferromagnetic order. The shallow peak in $\rho(T)$ at low temperatures in the sample with $x=0.2$ can be explained similar to that given by Gayathri et al. for maganites perovskites [41]. The sample ($x=0.2$) can be considered as a composite including both the metallic and semiconducting regions. The metallic behavior are mostly of com-

position close to $x=0$ sample. As the temperature is decreased the resistivity of the metallic regions reduces while that of the semiconducting regions increases. This tends to increase current paths through the metallic regions of low resistivity. Consequently, the conduction from the metallic regions predominates and resistivity decreases as the temperature is reduced. Thus, the shallow peak in resistivity signifies a crossover from metallic to semiconducting behaviors. However, for the samples with $x \geq 0.2$ the metallic regions make marginal contribution to conductivity even if they are present in small volume fractions. Further investigations on the magneto-transport properties of the $\text{Ba}_2\text{Fe}_{1-x}\text{Cr}_x\text{MoO}_6$ ($0 \leq x \leq 1$) double perovskite will be presented elsewhere.

4. Conclusions

We have made a systematic investigation of the effect of dilution of Fe^{3+} by Cr^{3+} on the magnetic, transport and magnetocaloric properties of the double perovskite $\text{Ba}_2\text{FeMoO}_6$. The substitution of Cr on the B-site cation (Fe) in series $\text{Ba}_2\text{Fe}_{1-x}\text{Cr}_x\text{MoO}_6$ ($0 \leq x \leq 1$) decreases the Curie temperature (from 340 K to 310 K for $x=0$ and 1, respectively) and the saturation magnetic moment, μ_s , from $3.63 \mu_B/\text{f.u.}$ for $x=0$ to $2.69 \mu_B/\text{f.u.}$ for $x=1$. It was found that Cr doping in the double perovskite $\text{Ba}_2\text{Fe}_{1-x}\text{Cr}_x\text{MoO}_6$ ($0 \leq x \leq 1$) reduces the maximum value of magnetic entropy change under low magnetic field. The maximum value of magnetic entropy change 2.08 J/kg K for $x=0$ at 1 T was found to be about 64% that of pure Gd, suggesting that these materials can be used as magnetic refrigerants near room temperature. A transition from metallic behavior at $x=0$ to semiconducting like behavior for all doped samples ($x \geq 0.2$) is observed.

Acknowledgement

The author would like to thank Technical University of Vienna (TU Wien), Vienna, Austria for the financial support during his stay.

References

- [1] G.A. Prinz, *Science* 282 (1998) 1660.
- [2] K.-I. Kobayashi, T. Kimura, Y. Tomioka, H. Sawada, K. Terakura, Y. Tokura, *Phys. Rev. B* 59 (1999) 11159.
- [3] A. Muñoz, J.A. Alonso, M.T. Casais, M.T. Martínez-Lope, M.T. Fernández-Díaz, *J. Phys.: Condens. Matter* 14 (2002) 8817.
- [4] G. Popov, M. Greenblatt, M. Croft, *Phys. Rev. B* 67 (2003) 024406.
- [5] A.K. Azad, S.G. Eriksson, A. Mellergad, S.A. Ivanov, J. Eriksen, R. Mathieu, P. Svedlindh, *Ferroelectric* 269 (2002) 105.
- [6] R.P. Borges, R.M. Thomas, C. Cullinan, J.M.D. Coey, R. Surya-narayanan, L. Bendor, L. Gaudart, A. Revcolevski, *J. Phys.: Condens. Matter* 11 (1999) 445.
- [7] A. Maignan, B. Raveau, C. Martin, M. Hervieu, *J. Solid State Chem.* 144 (1999) 224.
- [8] T. Horikubi, Kamegashira, *J. Alloys Compd.* 287 (1999) 62.
- [9] Y. Yasukawa, J. Linden, T.S. Chan, R.S. Liu, Yamauchi, Karppinen, *J. Solid State Chem.* 177 (2004) 2655.
- [10] K.-I. Kobayashi, T. Kimura, H. Sawada, K. Terakura, Y. Tokura, *Nature* 395 (1998) 677.
- [11] E.K. Hemery, G.V.M. Williams, J.D. Graham, H.J. Trodahl, *Curr. Appl. Phys.* 8 (2008) 273.
- [12] X.M. Feng, G.H. Rao, G.Y. Liu, H.F. Yang, W.F. Liu, Z.W. Ouyang, L.T. Yang, Z.X. Liu, R.C. Yu, C.Q. Jin, J.K. Liang, *J. Phys.: Condens. Matter* 14 (2002) 12503.
- [13] P.H. Shih, Y.Y. Fan, C.Y. Lee, W.T. Lai, H.C. Ku, H.Z. Chen, S.L. Young, *Physica B* 329 (2003) 731.
- [14] W. Zhong, N.J. Tang, X.L. Wu, W. Liu, W. Chen, H.Y. Jiang, Y.W. Du, *J. Magn. Magn. Mater.* 282 (2004) 151.
- [15] W. Zhong, W. Liu, X.L. Wu, N.J. Tang, W. Chen, C.T. Au, Y.W. Du, *Solid State Commun.* 132 (2004) 157.
- [16] A. Dhahri, J. Dhahri, S. Zemni, M. Oumezzine, H. Vincent, *J. Alloys Compd.* 420 (2006) 15.
- [17] F. Lümm, J.P. Wang, J.F. Liu, W. Song, X.F. Hao, D.F. Zhou, X.J. Liu, Z.J. Wu, J. Meng, *J. Phys.: Condens. Matter* 18 (2006) 1601.
- [18] A.P. Douvalis, T. Panagiotopoulos, V. Bakas, Papaefthymiou, *J. Magn. Magn. Mater.* 316 (2007) e940.
- [19] V. Pandey, V. Verma, R.P. Aloysius, G.L. Bhalla, V.P.S. Awana, H. Kishan, R.K. Kotnala, *J. Magn. Magn. Mater.* 321 (2009) 2239.

- [20] C. Ritter, M.R. Ibarra, L. Morellon, J. Blasco, J. Garca, J.M. De Teresa, J. Phys.: Condens. Matter 12 (2008) 295.
- [21] J. Kim, J.G. Sung, H.M. Yang, B.W. Lee, J. Magn. Magn. Mater. 290 (2005) 1009.
- [22] L. Balcells, J. Navarro, M. Bibes, A. Roig, B. Martinez, J. Fontcuberta, Appl. Phys. Lett. 78 (2000) 781.
- [23] A.S. Ogale, S.B. Ogale, R. Ramesh, T. Venkatesan, Appl. Phys. Lett. 75 (1999) 537.
- [24] J. Navarro, C. Frontear, L. Balcells, B. Martinez, J. Fontcuberta, Phys. Rev. B 64 (2001) 092411.
- [25] V.K. Pecharsky Jr., K.A. Gschneidner, J. Magn. Magn. Mater. 200 (1999) 44.
- [26] V.K. Pecharsky Jr., K.A. Gschneidner, J. Appl. Phys. 90 (2001) 4614.
- [27] M. El-Hagary, H. Michor, G. Hilscher, J. Magn. Magn. Mater., (2010), doi:10.1016/j.jmmm.2010.04.039.
- [28] M. El-Hagary, Y.A. Shoker, M. Emam-Ismail, A.M. Moustafa, A. Abd El Aal, A. Ramadan, Solid State Commun. 149 (2009) 184.
- [29] A.R. Dinesen, S. Linderroth, S. Morup, J. Phys: Condens. Matter 17 (2005) 6257.
- [30] W. Zhong, W. Chen, W.P. Ding, N. Zhang, Y.W. Du, Q.J. Yan, Solid State Commun. 06 (1998) 55.
- [31] Z.B. Guo, Y.W. Du, J.S. Zhu, H. Huang, W.P. Ding, D. Feng, Phys. Rev. Lett. 78 (1997) 1142.
- [32] W. Zhong, W. Chen, W.P. Ding, N. Zhang, A. Hu, Y.W. Du, Q.J. Yan, J. Eur. Phys. B 3 (1998) 169.
- [33] B.K. Banerjee, Phys. Lett. 12 (1964) 16.
- [34] M.H. Phan, H.X. Peng, S.C. Yu, N.D. Tho, H.N. Nhat, N. Chau, J. Magn. Magn. Mater. 316 (2007) e562.
- [35] M.H. Phan, T.L. Phan, S.C. Yu, N.D. Tho, N. Chau, Phys. Status Solidi (b) 241 (2004) 1744.
- [36] M.H. Phan, H.X. Peng, S.C. Yu, N.D. Tho, D.T. Hanh, N. Chau, J. Appl. Phys. 99 (2006) 08Q108.
- [37] Q.Y. Xu, K.M. Gu, X.L. Liang, G. Ni, J. Appl. Phys 1 (2001) 524.
- [38] M.H. Phan, S.B. Tian, D.Q. Hoang, S.C. Yu, C. Nguyen, A.N. Ulyanov, J. Magn. Magn. Mater. 258–259 (2003) 309.
- [39] K.A. Gschneidner Jr., V.K. Pecharsky, A.O. Tsokol, Rep. Prog. Phys. 68 (2005) 1479.
- [40] X.X. Zhang, J. Tajeda, Y. Xin, C.F. Sun, K.W. Wong, X. Bohigas, Appl. Phys. Lett. 69 (1996) 3596.
- [41] N. Gayathri, A.K. Raychauduri, S.K. Tiwary, R. Gundakaram, A. Arulraj, C.N.R. Rao, Phys. Rev. B 56 (1997) 1345.